Supplementary information of

Rapidly responsive liquid metal/polyimide photothermal actuators designed based on the bilayer structure's difference in coefficient of thermal expansion

Xiaofei Li[1, 2], Xin Ding [1], Yuhang Du[1, 2], Chao Xiao [1, 3], Yanyan Wang[1], Kang Zhen[1,3], Xianglan Liu[1], Lin Chen[1], Xingyou Tian[1, 2], Xian Zhang[* 1, 2, 3]

[1] Key Lab of Photovoltaic and Energy Conservation Materials, Institute of Solid State Physics, HFIPS, Chinese Academy of Sciences, Hefei 230031, China

[2] University of Science and Technology of China, Hefei 230026, China

[3] Lu'an Branch, Anhui Institute of Innovation for Industrial Technology, Lu'an 237100, China

*Corresponding authors at: 2221 Changjiang West Road, Shushan District, Hefei City, Anhui Province, People's Republic of China. E-mail addresses: xzhang@issp.ac.cn

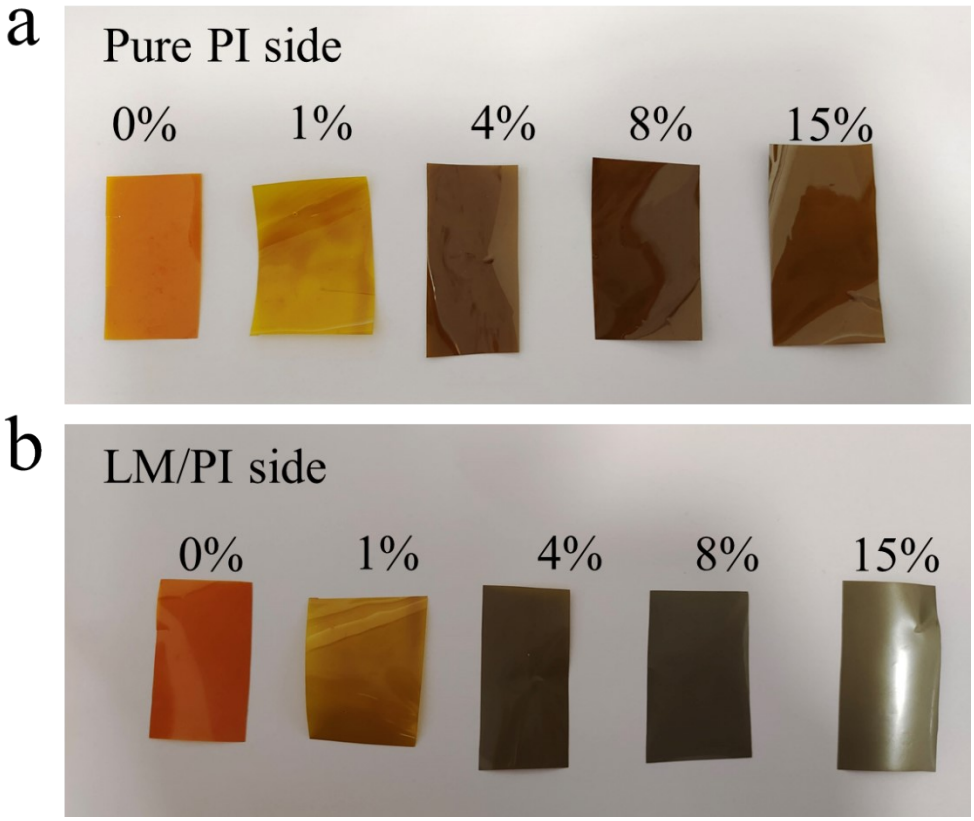

Figure S1 (a) The morphology of the pure PI side (close to the glass plate)of the photothermal actuator; (b) The morphology of the LM/PI side (exposure to air) of the photothermal actuator.

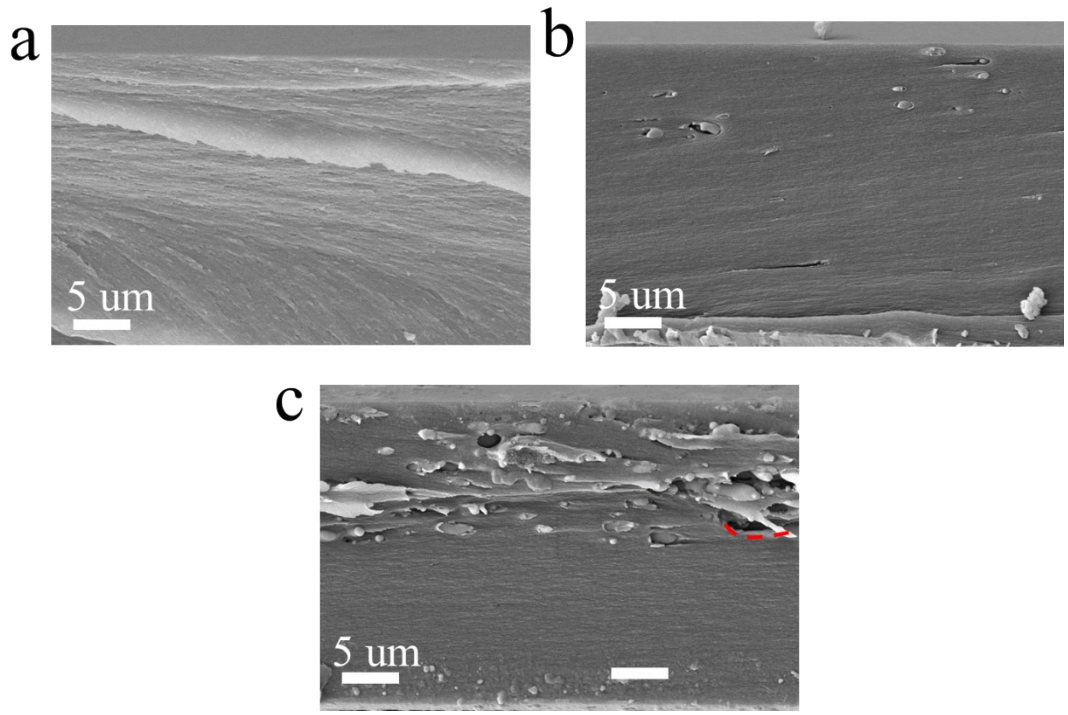

Figure S2 SEM image of (a) LM/PI-0%, (b) LM/PI-1%, (c) LM/PI-8% the photothermal actuator, LM particles are uniformly dispersed in PI.

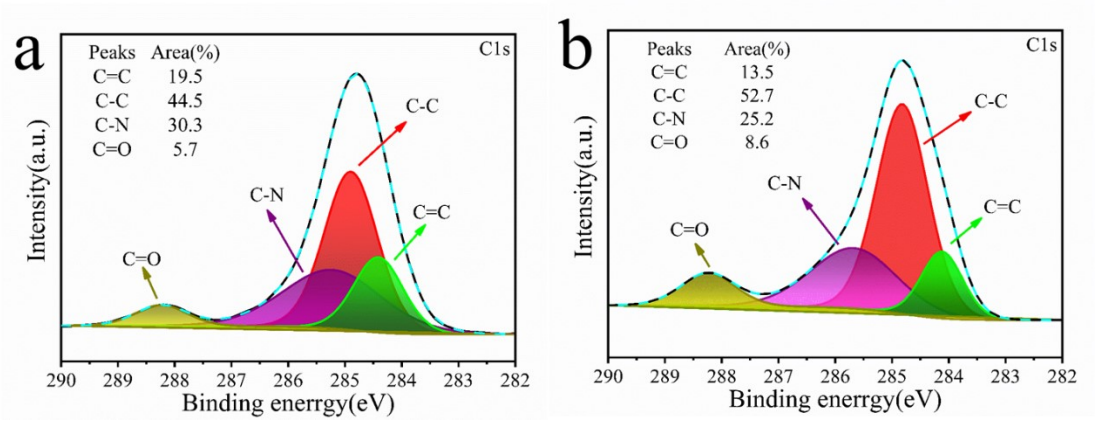

Figure S3 C1s narrow spectrum of (a) pure PI film and (b) LM/PI-4% photothermal actuator.

Table S1. Detailed data of linear fit of temperature laser power curves of LM/PI photothermal actuators

Equation	y = a + b×x				
LM Content	LM/PI-0%	LM/PI-1%	LM/PI-4%	LM/PI-8%	LM/PI-15%
a	7.55	-50.61	-138.41	-116.54	-118.20
b	24.44	119.51	265.34	223.95	235.70
R^2	0.9875	0.99712	0.99204	0.99493	0.99478

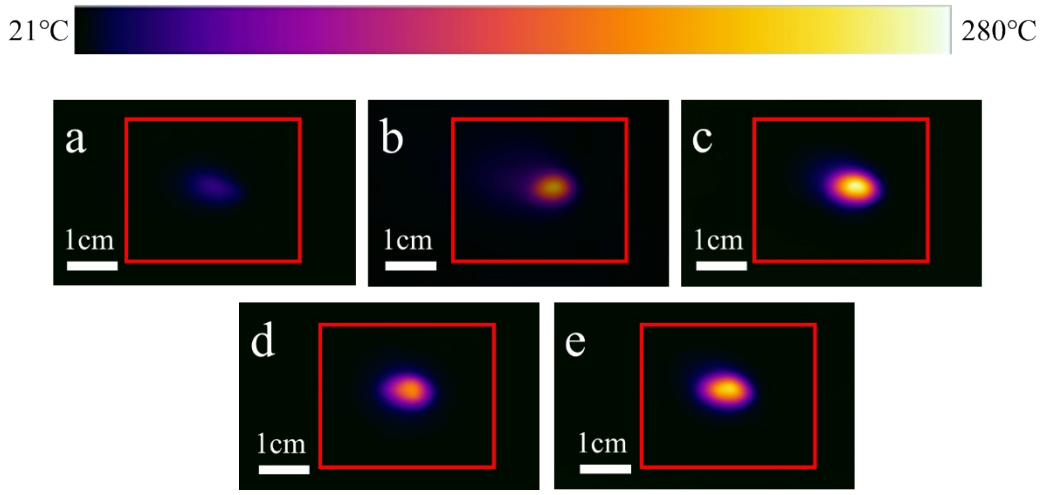

Figure S4 Infrared thermal image of (a) LM/PI-0%, (b) LM/PI-1%, (c) LM/PI-4%, (d) LM/PI-8%, (e) LM/PI-15% photothermal actuator at 1.5W/cm^2 NIR laser. The red box represents the size of the photothermal actuator.

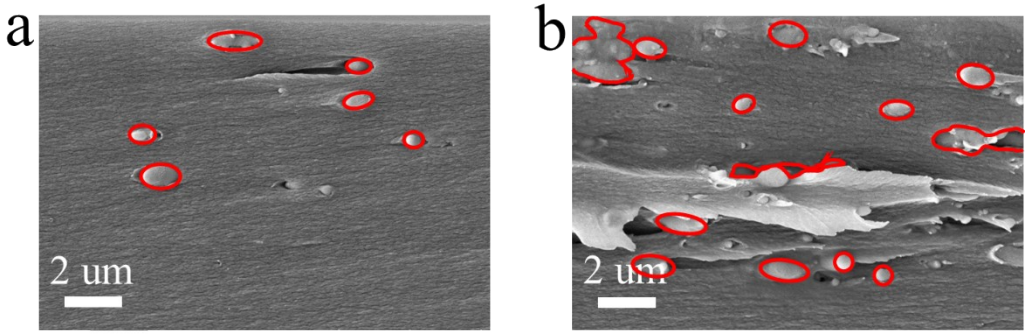

Figure S5 Morphology and size of LM particles in (a) LM/PI-1%, (b) LM/PI-8% photothermal actuator.

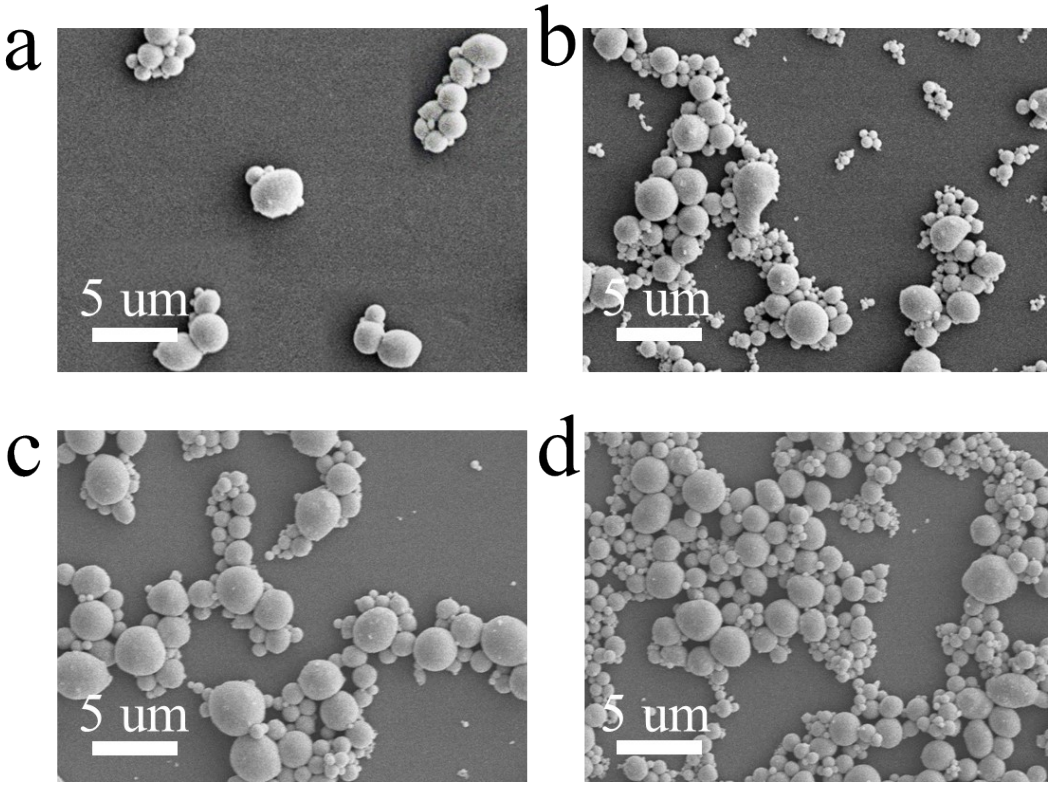

Figure S6 Morphology and size of LM with volume fraction (a) 1%, (b) 4%, (c) 8%, (d) 15% after 3min sonication.

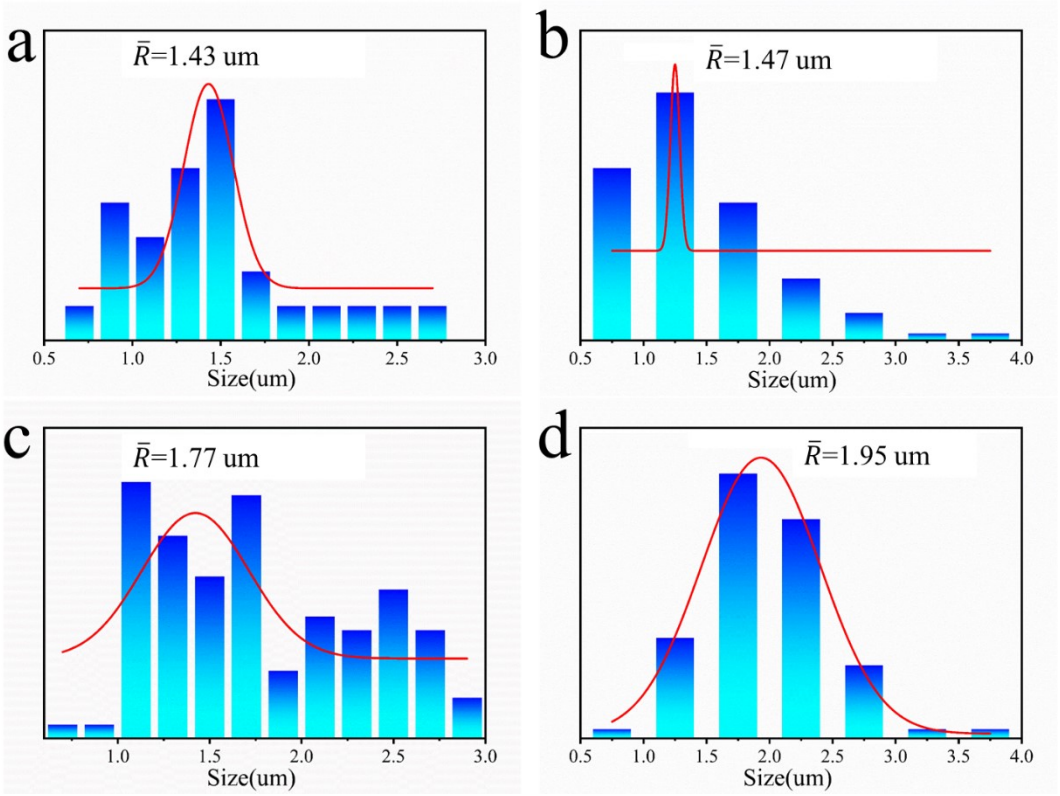

Figure S7 Distribution of LM particle size after ultrasonic min of LM with (a) 1%, (b) 4%, (c) 8%, (d) 15% volume fraction.

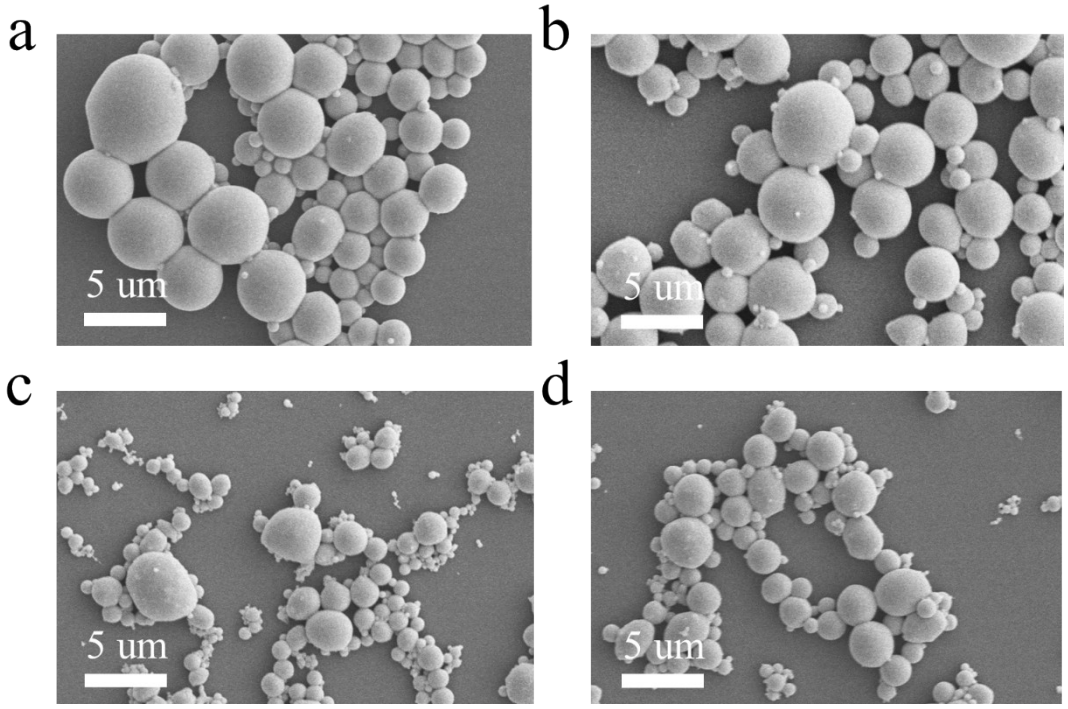

Figure S8 Morphology and size of LM with 4% volume fraction after (a) 30s, (b) 1 min, (c) 2 min, (d) 3 min of ultrasound.

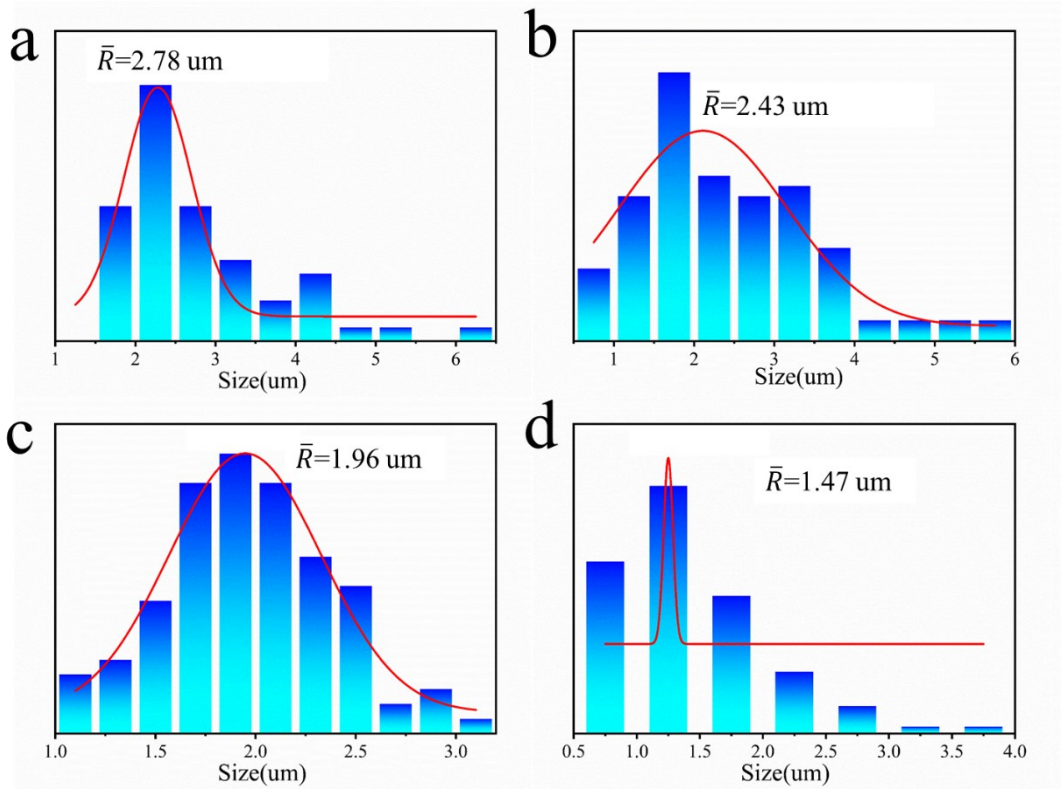

Figure S9 Distribution of LM particle size after (a) 30s, (b) 1min, (c) 2min, (d) 3min of ultrasound.

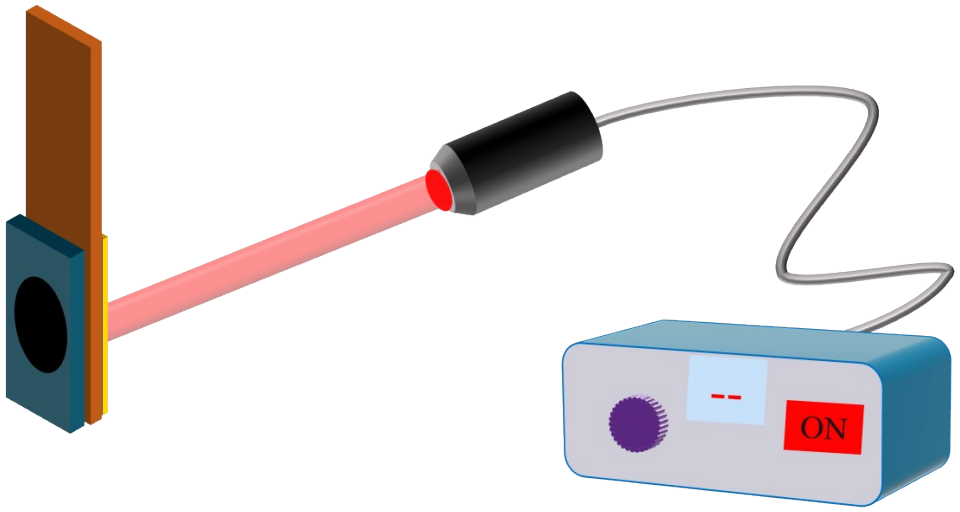

Figure S10 Schematic diagram of the LM/PI photothermal actuator heated copper plate.

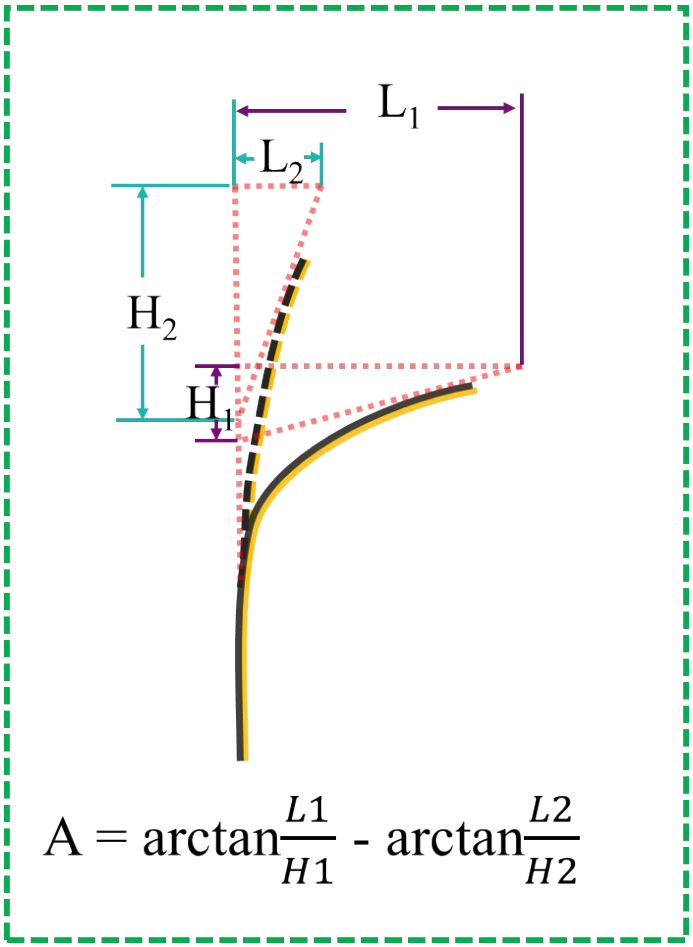

Figure S11 Calculation of bending angle of the photothermal actuator.

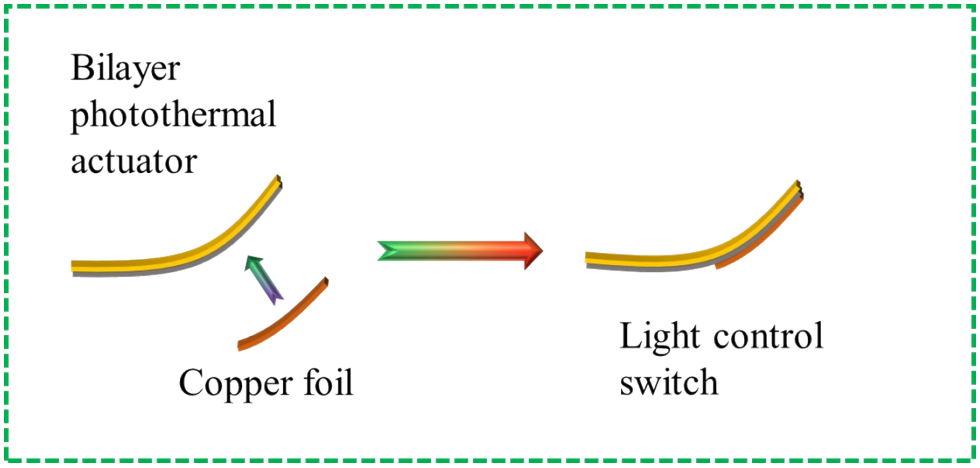

Figure S12 Schematic diagram of preparation of light control switch.

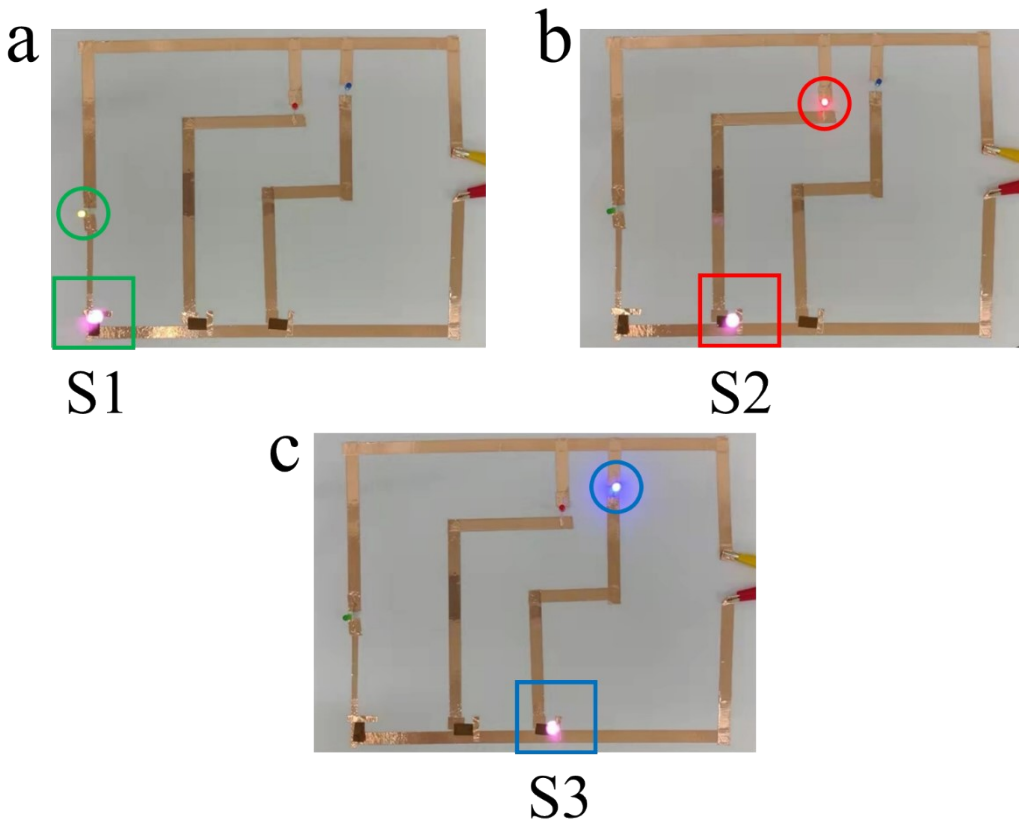

Figure S13 (a) The NIR laser irradiates to S1 and the green bulb lights up. (b) The NIR laser irradiates to S2 and the red bulb lights up. (c) The NIR laser irradiates to S1 and the blue bulb lights up.

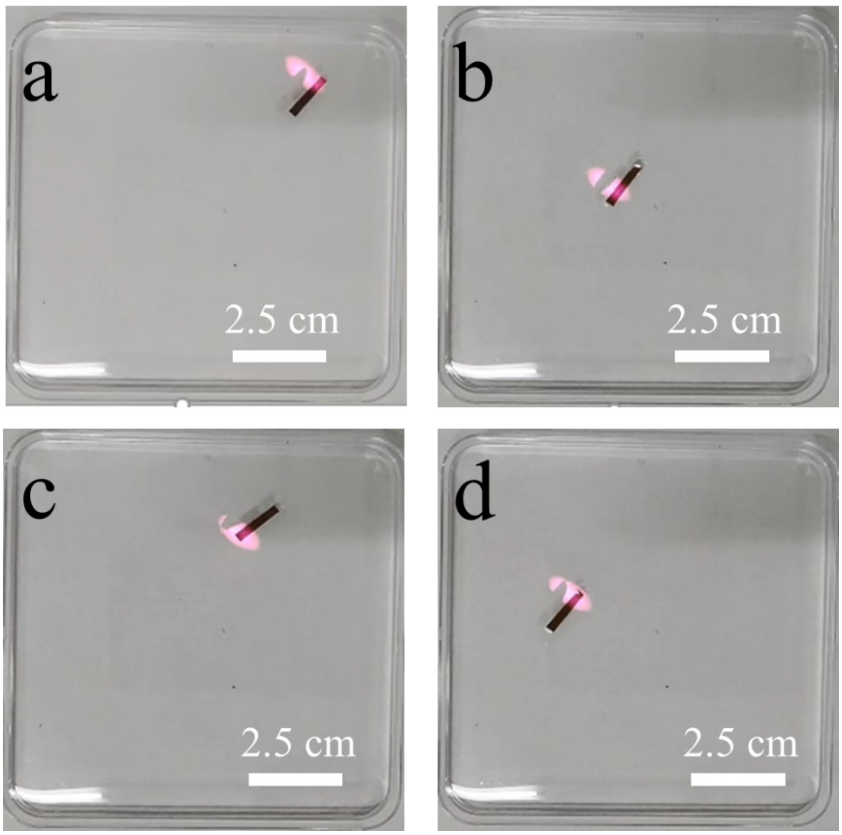

Figure S14 The NIR laser can control the direction of the photothermal actuator swim.

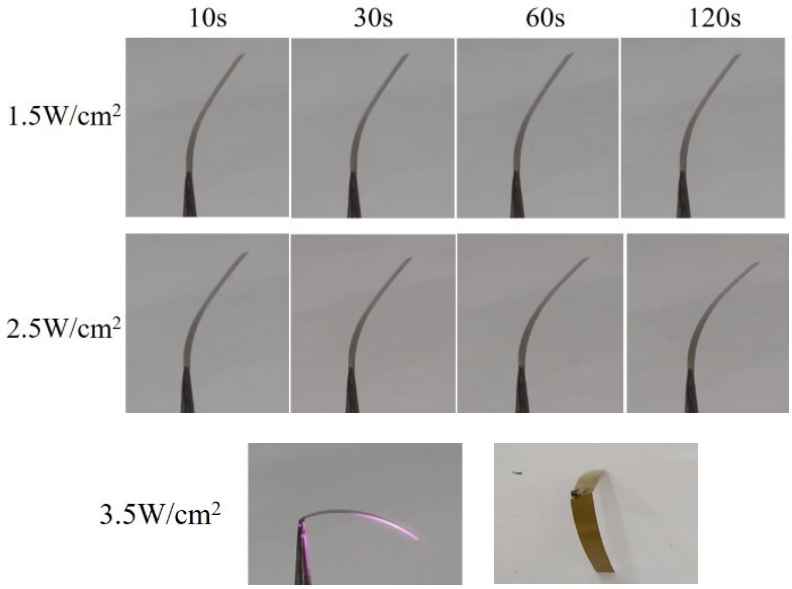

Figure S15 Bending angle of LM/PI-4% photothermal actuator after different irradiation times under 1.5 W/cm2, 2.5 W/cm2, 3.5 W/cm^2 NIR laser.

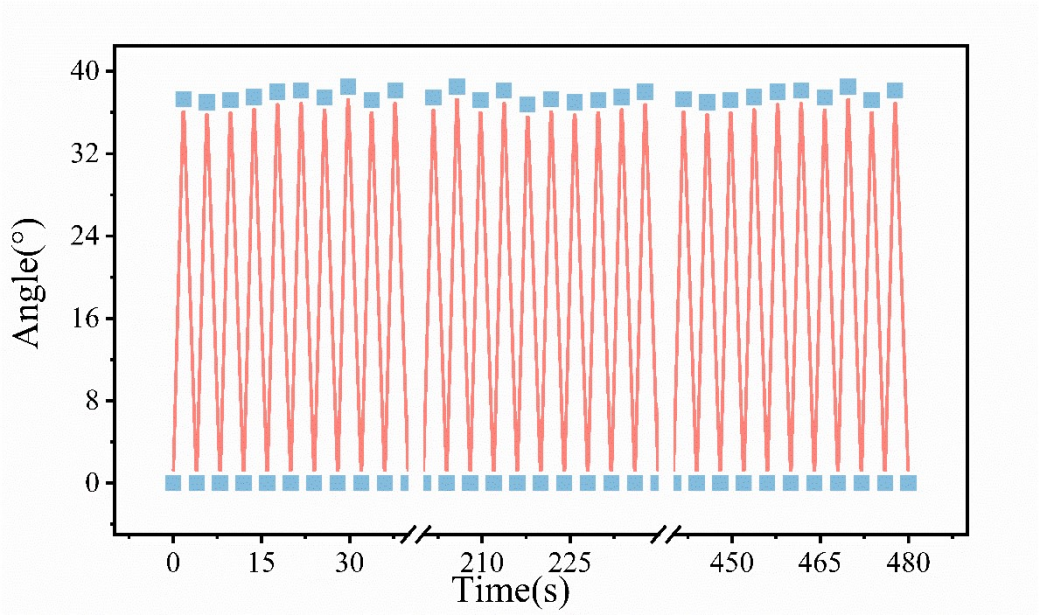

Figure S16 The LM/PI-8% photothermal actuator can easily cycle 120 times under 1.5 W/cm^2 NIR laser.